

CONTRIBUTION FROM STAR-FORMING GALAXIES TO THE COSMIC GAMMA-RAY BACKGROUND RADIATION

RYU MAKIYA AND TOMONORI TOTANI

Department of Astronomy, Kyoto University, Kitashirakawa-Oiwake-cho, Sakyo-ku, Kyoto 606-8502, Japan

AND

MASAKAZU A. R. KOBAYASHI

National Astronomical Observatory of Japan, 2-21-1 Osawa, Mitaka, Tokyo, 181-8588, Japan

Draft version March 5, 2022

ABSTRACT

We present a new theoretical calculation of the contribution to the extragalactic gamma-ray background radiation (EGRB) from star-forming galaxies, based on a state-of-the-art model of hierarchical galaxy formation that is in quantitative agreement with a variety of observations of local and high-redshift galaxies. Gamma-ray luminosity (L_γ) and spectrum of galaxies are related to star formation rate (ψ), gas mass (M_{gas}), and star formation mode (quiescent or starburst) of model galaxies using latest observed data of nearby galaxies. We try the two limiting cases about gamma-ray production: the escape limit ($L_\gamma \propto \psi M_{\text{gas}}$) and the calorimetric limit ($L_\gamma \propto \psi$), and our standard model predicts 7 and 4% contribution from star-forming galaxies to the total EGRB flux (including bright resolved sources) recently reported by the *Fermi* Gamma-Ray Space Telescope. Systematic uncertainties do not allow us to determine the EGRB flux better than by a factor of ~ 2 . The predicted number of nearby galaxies detectable by *Fermi* is consistent with the observation. Intergalactic absorption by pair-production attenuates the EGRB flux only by a modest factor of ~ 1.3 at the highest *Fermi* energy band, and the reprocessed cascade emission does not significantly alter EGRB at lower photon energies. The sum of the known contributions from AGNs and star-forming galaxies can explain a large part of EGRB, with a remarkable agreement between the predicted model spectrum and observation.

Subject headings: cosmic rays — diffuse radiation — galaxies: evolution — gamma rays : theory

1. INTRODUCTION

The existence of the extragalactic diffuse gamma-ray background (EGRB) has been revealed first by the SAS-2 satellite (Fichtel et al. 1977; Fichtel et al. 1978). Better determinations of the flux and spectrum of EGRB were achieved by the EGRET detector on board the Compton Gamma-Ray Observatory (Sreekumar et al. 1998; Strong et al. 2004a). The most reliable measurement of EGRB has very recently been reported based on the data of the *Fermi* Gamma-Ray Space Telescope (Atwood et al. 2009), and the EGRB spectrum is well described by a single power-law with a photon index of 2.41 ± 0.05 and the photon flux of about $(1.03 \pm 0.17) \times 10^{-5}$ photons $\text{cm}^{-2} \text{s}^{-1} \text{sr}^{-1}$ above 100 MeV (Abdo et al. 2010c).

The origin of EGRB has been discussed for a long time and various sources have been discussed as possible contributors to EGRB, such as active galactic nuclei (AGNs, especially blazars), galaxy clusters, intergalactic shocks produced by structure formation, and dark matter annihilation (see, e.g., Dermer 2007 for a review).

Almost all of the known extragalactic gamma-ray sources are blazars, and their contribution to the EGRB has been intensively studied (e.g., Inoue & Totani 2009; Venters 2010; Abdo et al. 2010d, and references therein). However, star-forming galaxies should also be gamma-ray emitters by cosmic-ray interactions with interstellar medium (ISM) and interstellar radiation field (ISRF) (Strong et al. 2000; Strong et al. 2004b), and there must be non-zero contribution to EGRB. This is obvious because we know that the Galactic disk is a strong source of diffuse gamma-rays, and gamma-rays from Large Magellanic Cloud (LMC) have

been detected by EGRET (Sreekumar et al. 1992). Furthermore, gamma-ray emission in GeV–TeV from Small Magellanic Cloud (SMC, Abdo et al. 2010e) and two nearby starburst galaxies, M82 and NGC 253, have recently been discovered by H.E.S.S. (Acero et al. 2009), VERITAS (VERITAS Collaboration 2009), and *Fermi* (Abdo et al. 2010a). The purpose of this paper is to present a new estimate of the contribution from star-forming galaxies to EGRB.

There are a number of previous studies on this issue (Strong et al. 1976; Lichti et al. 1978; Dar & Shaviv 1995; Pavlidou & Fields 2002; Thompson et al. 2007; Bhattacharya & Sreekumar 2009; Ando & Pavlidou 2009; Lacki et al. 2010; Fields et al. 2010), and the estimates of the contribution to EGRB ranges ~ 10 –50%¹. Most of these studies calculated gamma-ray luminosity (L_γ) from star formation rate (SFR) of galaxies, because the cosmic-ray energy input is expected to be proportional to SFR. However, if escape of cosmic-rays from galaxies is significant, SFR cannot be used as a reliable indicator of L_γ (see §2.2 in more details). Several studies used infrared luminosity of galaxies as SFR indicators, but IR luminosity (especially at far-IR in early-type galaxies) is not a perfect SFR estimator because a significant amount of dust can be heated by ISRF from relatively old stars (e.g., Salim et al. 2009 and references therein).

Amount of interstellar gas should also be important to determine L_γ , because the degree of cosmic-ray escape is af-

¹ Here, the contribution is against the total (physical) extragalactic background photon flux (> 100 MeV) including bright resolved sources. It is often calculated against the unresolved component of EGRB, but it depends on the flux sensitivity of a particular detector. Throughout the paper, “the contribution to EGRB” is defined against the total EGRB flux, which we estimated from the resolved and unresolved components of the *Fermi* data (Abdo et al. 2010d). We used a photon index of 2.4 for resolved blazars (Abdo et al. 2010d) to extrapolate the resolved component from 200 to 100 MeV.

ected by the target amount. In fact, recent observations indicate that gamma-ray luminosity is nicely correlated with the product of SFR and gas mass in galaxies (Abdo et al. 2010a). Pavlidou & Fields (2002) included gas mass in the theoretical prediction of EGRB using the data of the cosmic star formation history (CSFH). Galaxies in the universe is considered as a closed box containing stellar and gas mass in present-day galaxies, and CSFH is used to solve the time evolution of relative fractions of stars and gas. However this approach likely overestimates the gas mass contributing to gamma-ray production at high redshifts, because most of the present-day stellar mass is in the form of gas and assumed to contribute to gamma-ray emission. In reality, only the gas in collapsed dark halos can contribute to cosmic-ray interactions in galaxies, which is a small fraction at high redshifts according to the structure formation theory. Recently, Fields et al. (2010) incorporated gas mass in galaxies using the Schmidt-Kennicutt relation in their calculation of EGRB. In this case one must know galaxy size to relate SFR and M_{gas} , and a single value of galaxy size at each redshift was assumed as a simple model.

Here we present a new calculation of the contribution from star-forming galaxies in EGRB using a state-of-the-art theoretical model of galaxy formation in the framework of hierarchical galaxy formation, which is in quantitative agreement with a variety of observations at high redshifts as well as the local universe. An advantage of our approach compared with previous studies is that we can calculate both SFR and gas mass of individual galaxies at various redshifts. Furthermore, we utilize the information of the gamma-ray spectra recently observed for nearby starbursts, in addition to the standard spectrum of the Galactic diffuse emission, to predict the EGRB spectrum based on the galaxy formation model including both quiescent and starburst galaxy populations.

The paper is organized as follows. In the next section we describe our model calculations. We present the results on EGRB and statistics about the number of nearby galaxies detectable by *Fermi* in §3. After discussion on the uncertainties in our calculation (§4.1) and implications for the origin of EGRB (§4.2), conclusions will be presented in §5. In this work, cosmological parameters of $\Omega_0 = 0.3$, $\Omega_\Lambda = 0.7$, and $H_0 = 70 \text{ Mpc}^{-1} \text{ km s}^{-1}$ are adopted.

2. FORMULATIONS

2.1. The Theoretical Model of Hierarchical Galaxy Formation

We use a mock numerical galaxy catalog produced by one of the latest so-called semi-analytic models (SAMs) of hierarchical galaxy formation [the Mitaka model (Nagashima & Yoshii 2004; Nagashima et al. 2005)]. In general, SAMs compute merging history of dark matter (DM) halos based on the standard structure formation theory driven by cold dark matter, and include several important physical processes related to the evolution of baryons in DM halos such as radiative gas cooling, star formation, supernova feedback, galaxy merger, stellar population synthesis, chemical evolution, and extinction by interstellar dust (e.g., Kauffmann et al. 1993; Cole et al. 1994; Nagashima et al. 1999; Somerville & Primack 1999; Baugh et al. 2005). In each time step of the halo merging history, two discrete modes of star formation are considered in the model, i.e., starburst and quiescent. When galaxies experience a major galaxy merger, intensive burst of star formation is assumed to occur (the starburst mode), and all of the available cold gas is con-

verted into stars and hot gas within a short time. Otherwise star formation proceeds at a modest rate determined by cold gas amount and dynamical time scales (the quiescent mode).

The Mitaka model can quantitatively reproduce a wide variety of observed characteristics of local galaxies, including luminosity functions (LFs) and scaling relations among various observables such as magnitude, colors, surface brightness, size, gas mass-to-light ratio, and metallicity (Nagashima & Yoshii 2004). Moreover, it can also reproduce well the cosmic star formation history (Nagashima & Yoshii 2004), the rest-frame ultraviolet (UV) continuum LF of Lyman break galaxies at $z = 4$ and 5 (Kashikawa et al. 2006), and all of the available observations for the high- z Ly α emitters (Ly α and UV continuum LFs, and Ly α equivalent width distributions) (Kobayashi et al. 2007, 2010).

In the version of the Mitaka model used here, about 100 Monte-Carlo realizations of merger histories are produced for DM halos in a DM mass interval of 0.1 dex at each output redshift ranging $z = 0$ –10. The model calculates DM halos with velocity dispersions larger than 30 km/s, and this allows us to make a reliable prediction in the stellar mass range of $\gtrsim 10^6 M_\odot$, roughly corresponding to the absolute B band magnitude of $M_B \lesssim -10$ mag.

2.2. Modeling Gamma-Ray Emission from Galaxies

To calculate the EGRB flux from normal galaxies, we need the gamma-ray LF $\phi(L_\gamma, z)$ (comoving number density of galaxies per unit gamma-ray luminosity) as a function of redshift. Here, L_γ is defined as gamma-ray luminosity in the rest-frame photon energy range of 0.1–5 GeV. The LF ϕ is calculated from the mock galaxy catalog by modeling gamma-ray luminosity of each galaxy as follows.

Diffuse gamma-ray radiation in galaxies is produced by the interactions between the cosmic-rays and ISM. If the cosmic-ray losses are dominated by escape, the gamma-ray luminosity is set by equilibrium between cosmic ray production and escape. It is then expected that gamma-ray luminosity depends on SFR (ψ , an indicator of cosmic ray production rate) and mass of interstellar gas (M_{gas} , the amount of target for cosmic rays to interact before escape), i.e., $L_\gamma \propto \psi M_{\text{gas}}$. We call it “the escape limit”. However, if the cosmic-ray energy losses are dominated by inelastic collision with interstellar gas and almost all of the cosmic-ray energy is converted into gamma-rays, the gamma-ray luminosity is no longer dependent on the amount of gas, i.e., $L_\gamma \propto \psi$. We call it “the calorimetric limit”. [See also Pavlidou & Fields (2001), Torres et al. (2004), and Thompson et al. (2007) for more discussion on this issue.] Since it is difficult to model the detailed escape and energy loss processes of cosmic-rays in galaxies, we consider both of these two simple limiting cases.

To establish the link between L_γ and ψ and/or M_{gas} , we collected the observed values of these quantities for the nearby galaxies of SMC, LMC, the Milky Way (MW), M82, and NGC 253. They are summarized in Table 1. For SMC and LMC, SFRs are estimated from H α luminosities (Kennicutt et al. 2008), using the relationship of Kennicutt (1998) assuming the Salpeter initial mass function (IMF) in 0.1–100 M_\odot . Extinction by dust is not taken into account, and the uncertainty about this will be discussed later (§4.1). For M82 and NGC 253, we used SFR estimated from the IR luminosity from interstellar dust, using the relationship of Kennicutt (1998) assuming the same IMF as above, since these galaxies has large extinction (Dale et al. 2007 and Pence 1980) and H α is no longer a good indicator of SFR. To-

total IR luminosity is calculated from the IRAS fluxes in the three bands (Sanders et al. 2003) using the formula given in Dale & Helou (2002). Since it is difficult to estimate the total IR luminosity of MW, we use the supernova rate estimated by a gamma-ray observation (Diehl et al. 2006) and converted it into SFR assuming the same IMF. The standard value of $8 M_\odot$ is adopted for the mass threshold of core-collapse supernova explosions.

The gas mass is estimated by the total of H_2 and $H\ I$, where the former and the latter are measured by CO and 21-cm line observations, respectively. The references are shown in Table 1. There are various estimations for $H\ I$ mass of SMC and LMC by different authors (Huchtmeier & Richter 1989, Stanimirović et al. 1999, Brüns et al. 2005 for SMC, and Huchtmeier & Richter 1989, Luks & Rohlf's 1992, Westerlund 1997, Staveley-Smith et al. 2003, Brüns et al. 2005 for LMC). Here we adopted the latest value by Brüns et al. (2005), and the standard deviations of the $H\ I$ mass measurements among difference papers were added to the errors as a quadratic sum, to take into account the uncertainty (Table 1).

The collected data are plotted in Figure 1. It is clearly seen that there is a good correlation both for the L_γ - ψM_{gas} (top panel) and L_γ - ψ relations (bottom panel). We fitted these relations by a single power-law function to the data points of SMC, LMC, M82, and NGC 253, and the results are

$$L_\gamma = (0.28 \pm 0.07) \times \left(\frac{\psi}{M_\odot \text{ yr}^{-1}} \times \frac{M_{\text{gas}}}{10^9 M_\odot} \right)^{0.86 \pm 0.06} [10^{39} \text{ erg/s}] \quad (1)$$

and

$$L_\gamma = (0.46 \pm 0.12) \times \left(\frac{\psi}{M_\odot \text{ yr}^{-1}} \right)^{1.2 \pm 0.09} [10^{39} \text{ erg/s}], \quad (2)$$

where the errors are statistical 1σ . In the fitting calculation we adopted the effective variance method which takes into account the errors of both coordinates (Orear 1981). Since SFR of MW has a large uncertainty, we did not use the data of MW in the fitting, although it is consistent with the correlation. The exact proportionality between L_γ and ψM_{gas} or L_γ and ψ are not necessarily expected, because it depends on propagation and degree of confinement of cosmic rays within a galaxy. Therefore we use these power-law relation to calculate gamma-ray luminosity. The cases of the exact proportionality, i.e., $L_\gamma \propto (\psi M_{\text{gas}})^1$ and $L_\gamma \propto (\psi)^1$ will also be discussed later (§4.1).

It should be noted that M_{gas} in the Mitaka model has been compared with observations of local galaxies as a function of B band galaxy luminosity (Nagashima & Yoshii 2004; Nagashima et al. 2005), showing a good agreement. This gives a support to apply M_{gas} of the Mitaka model to the L_γ - ψM_{gas} relation determined by observations, though the model has not yet been tested against M_{gas} at high redshifts because only very few observations are available. As for SFR, the adopted IMF in the Mitaka model (the Salpeter in 0.1 – $60 M_\odot$) is slightly different from that (in 0.1 – $100 M_\odot$) assumed in converting the observed IR luminosity to SFR in Fig. 1. Though the value of SFR is hardly affected by the upper bound of stellar mass in IMF, it may affect the conversion from IR luminosity to SFR. However we confirmed, using the PEGASE stellar library (Fioc & Rocca-Volmerange 1997), that the dif-

ference of the IMF mass ranges hardly affects the total luminosity from young stars because stars heavier than $60 M_\odot$ are scarce and have short lifetimes. It is negligible at the stellar population ages larger than $10^{6.5}$ yrs, and at most 20% at ages younger than that. Therefore we can apply SFRs in the Mitaka model to the fitting formula eqs. (1) and (2).

2.3. Gamma-Ray Spectra of Galaxies

We also need to model the gamma-ray spectrum of galaxies to predict the EGRB spectrum. The observed gamma-ray spectra of MW, M82, and NGC 253 are shown in Figure 2. We simply assume that quiescent galaxies have the same spectral shape as that of MW. For the MW spectrum we used the GALPROP fit to the *Fermi* spectral data of the Galactic diffuse gamma-rays (Abdo et al. 2010c). The observed spectrum of SMC and LMC are similar to that of MW.

For starburst galaxies, we expect some change of gamma-ray spectrum by the following physical reason. Because of the high density of star forming regions, it is plausible that starburst galaxies are ‘‘calorimetric’’ and have harder spectrum than quiescent galaxies because of less significant escape of high energy cosmic rays. Therefore we apply two modelings for the starburst spectra: (1) starbursts have the same spectrum as MW, and (2) the MW-like spectrum at low energy range and a hard power-law tail at high energy range. We fitted the spectrum of M82 and NGC 253 by the MW spectrum at energy less than 10 GeV, and with power law above the 10 GeV. Normalization of the power law component was determined so that it smoothly connects to the MW spectrum at 10 GeV. (Therefore the free parameters of the fit are two: the normalization of MW component and the photon index of high-energy power-law component.) As a result of the fitting, we find that M82 and NGC 253 can be fit with almost the same photon index of 2.2, and hence we adopt this spectrum when we try a different spectrum from MW for starburst galaxies². These model spectra are shown in Figure 2.

2.4. The EGRB Calculation

Given the modeling of gamma-ray luminosity of galaxies described above, the EGRB flux and spectrum can be calculated by integrating the gamma-ray luminosity function $\phi(L_\gamma, z)$ over redshift. To see the redshift evolution of the gamma-ray emissivity, we show the redshift evolution of ρ_ψ (comoving SFR density, proportional to gamma-ray luminosity density \mathcal{L}_γ in the calorimetric limit) as well as $\rho_{\psi M}$ (the comoving density of ψM_{gas} , proportional to \mathcal{L}_γ in the escape limit) in Figure 3. This figure indicates that $\rho_{\psi M}$ decreases more rapidly toward higher redshift than ρ_ψ , and this is likely because ψ is roughly proportional to M_{gas} and hence both the cosmic densities of ψ and M_{gas} decrease to high redshift beyond $z \sim 1$.

Given the gamma-ray luminosity function of galaxies $\phi(L_\gamma, z)$, the EGRB spectrum (photon flux per unit photon energy per steradian) is expressed as

$$\frac{d^2 F(\epsilon_\gamma)}{d\epsilon_\gamma d\Omega} = \frac{c}{4\pi} \int_0^{z_{\text{max}}} \left| \frac{dt}{dz} \right| dz \int_0^\infty dL_\gamma \phi(L_\gamma, z) \times (1+z) \frac{dL_\gamma [L_\gamma (1+z) \epsilon_\gamma]}{d\epsilon_{\gamma,r}} e^{-\tau_\gamma(z, \epsilon_\gamma)}, \quad (3)$$

where ϵ_γ is photon energy for observers at $z = 0$, t the cosmic

² In the spectral fitting, we ignored the data points that have only upper limits.

Table 1
Summary of L_γ , SFR, M_{gas} , and Distance of Nearby Galaxies

| Object | L_γ^a [10^{39} erg/s] | SFR ^b [M_\odot/yr] | M_{gas}^c [$10^9 M_\odot$] | Distance ^d [Mpc] |
|---------|------------------------------------|---------------------------------------------|------------------------------------------|--------------------------------|
| SMC | 0.011 ± 0.001 | 0.037 ± 0.011 | 0.45 ± 0.11 | 0.061 ± 0.003 |
| LMC | 0.041 ± 0.007 | 0.244 ± 0.073 | 0.56 ± 0.14 | 0.049 ± 0.001 |
| M82 | 13.0 ± 5.0 | 16.3 ± 2.4 | 4.9 ± 0.58 | 3.6 ± 0.3 |
| NGC 253 | 7.2 ± 4.7 | 7.9 ± 4.9 | 4.3 ± 0.55 | 3.9 ± 0.4 |
| MW | 3.2 ± 1.6 | 2.6 ± 1.5 | 7.0 ± 1.0 | – |

^aGamma-ray luminosities are in 0.1–5 GeV, from Abdo et al. (2010e) for SMC, Abdo et al. (2010b) for LMC, and Abdo et al. (2010a) for M82, NGC 253 and MW.

^bSee text (§2.2) for methods and references of SFR estimates.

^cTotal gas mass ($\text{H I} + \text{H}_2$) are estimated from 21-cm and CO line fluxes. References are Weiß et al. (2005), Huchtmeier & Richter (1989) (for M82), Knudsen et al. (2007), Springob et al. (2005) (for NGC 253), and Boissier & Prantzos (1999) (for MW). For SMC and LMC, see text (§2.2) for methods and references of gas mass estimates.

^dReferences are Hilditch et al. (2005) for SMC, Pietrzyński et al. (2009) for LMC, Freedman et al. (1994) for M82, and Karachentsev et al. (2003) for NGC 253.

time, and dt/dz can be calculated if the standard cosmological parameters are given. The rest-frame gamma-ray spectrum of galaxies $dL_\gamma(L_\gamma, \epsilon_{\gamma,r})/d\epsilon_{\gamma,r}$ can be calculated for a given L_γ by the spectral shapes as modeled in the previous section, where $\epsilon_{\gamma,r}$ is a photon energy at the rest-frame of the source redshifts. We set the maximum redshift $z_{\text{max}} = 10$ corresponding to that of the galaxy formation model, but this parameter hardly affects the EGRB flux because the majority of the EGRB flux comes from galaxies at $z \lesssim 2$ (see §3 below).

High energy photons ($\gtrsim 20$ GeV) are absorbed during the propagation in intergalactic space, by interaction with the cosmic infrared background (CIB) photons producing electron-positron pairs (Salamon & Stecker 1998; Totani & Takeuchi 2002; Kneiske et al. 2004; Stecker et al. 2006). The optical depth $\tau_\gamma(z, \epsilon_\gamma)$ in equation (2) represents this interaction. Since the infrared emission from dust has not yet been included in the Mitaka model, τ_γ cannot be calculated self-consistently based on the Mitaka model. Therefore we use the model of Totani & Takeuchi (2002) for τ_γ in this work, which is based on a different galaxy evolution model. To examine the effect of the uncertainty about τ_γ , we also calculated with different models of τ_γ by Kneiske et al. (2004) and Franceschini et al. (2008), and found that the change in the EGRB flux is not significant (negligible at $\lesssim 30$ GeV, and at most by a factor of 1.5 at the highest *Fermi* energy band).

The created pairs would scatter up the cosmic microwave background photons to gamma-rays via inverse Compton mechanism (cascade emission) and they make some contributions to the EGRB flux at lower photon energies (Aharonian et al. 1994; Fan et al. 2004). We calculate the contribution from the cascade emission using the same formalism of Kneiske & Mannheim (2008).

3. RESULTS

3.1. EGRB Predictions Compared with Observation

Figure 4 shows the quiescent and starburst components of EGRB calculated by the formulations presented in the previous section, for the two different modelings of the escape and calorimetric limits in different two panels. The data points are the *Fermi* measurements of EGRB flux (Abdo et al. 2010c). The reported *Fermi* EGRB spectrum is the residual after the

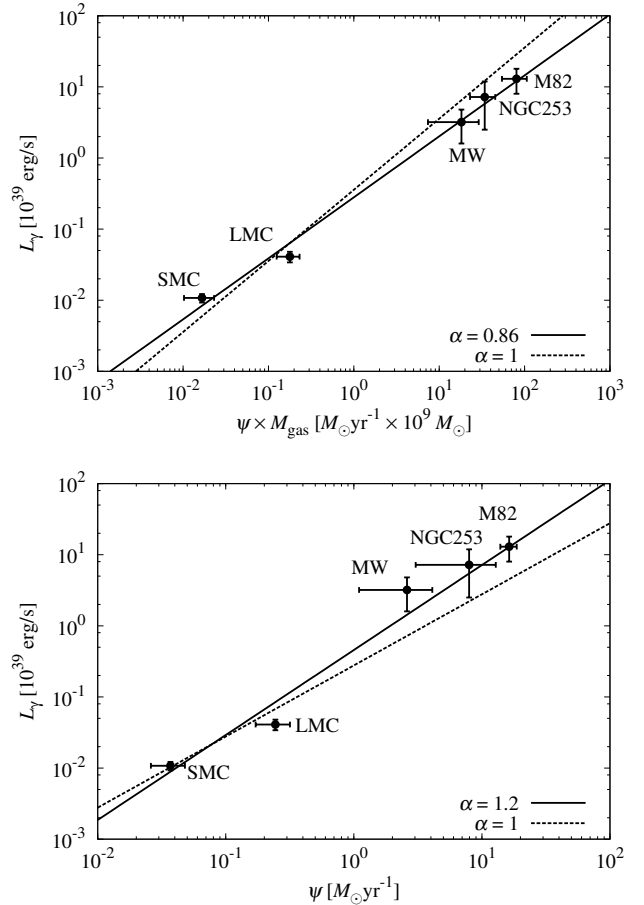


Figure 1. (Top) Correlation between the gamma-ray luminosity L_γ (0.1–5 GeV) and the product of SFR and gas mass, ψM_{gas} . The solid line represents the best fit power-law $L_\gamma \propto (\psi M_{\text{gas}})^\alpha$ with α taken as a free parameter. The dashed line represents a linear function fit with a fixed value of $\alpha = 1$. (Bottom) The same as top panel, but for the correlation between L_γ and SFR.

sources resolved by *Fermi* have been subtracted, and it is difficult to compare a theoretical prediction to such data taking into account complicated detection process and efficiencies. Therefore we also plot the total *Fermi* EGRB flux including the contribution from resolved sources as reported by Abdo et al. (2010c), and compare our prediction including all sources in the universe with this total observed flux. For the starburst galaxies we plotted the two models using the two different spectral shapes (MW or MW+power-law) as discussed in §2.3. All the predictions take into account the intergalactic absorption and the reprocessed cascade emission as discussed in the previous section.

In Figure 5, the predictions of total EGRB flux from all star-forming galaxies (quiescent plus starburst) are plotted. To show the effect of intergalactic absorption, the EGRB spectrum without taking into account the absorption is also plotted. The cascade component produced by the absorption is also shown. It can be seen that the intergalactic absorption attenuates the EGRB flux by a factor of about 1.3 at the highest photon energy of *Fermi*. The fraction of the absorbed energy flux of EGRB is not a large amount compared with the total EGRB energy flux, and hence the cascade component does not make a significant contribution at the low energy bands (Note that Fig. 5 is made as a νF_ν plot).

The EGRB flux from starburst galaxies is significantly en-

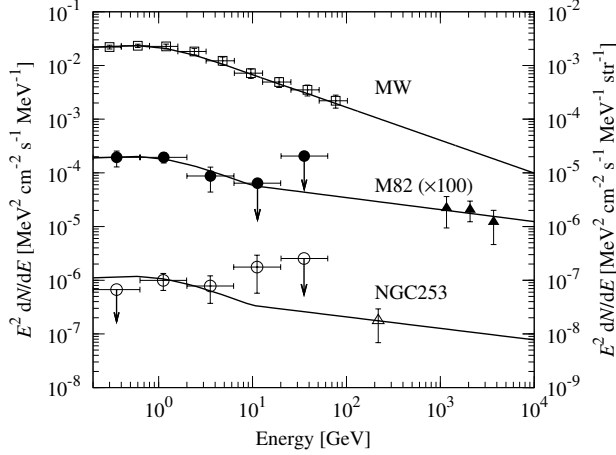


Figure 2. The gamma-ray spectrum $E^2 dN/dE$ of MW, M82 and NGC 253, where E is gamma-ray energy and dN/dE the differential photon flux. The MW spectrum is diffuse background flux in units shown on the right ordinate, and the others are flux from a source in units shown on the left ordinate. For the purpose of presentation, the spectrum and the data points of M82 are multiplied by 100. The MW data (open squares) are the Galactic diffuse gamma-rays averaged over $|b| > 10^\circ$ (Abdo et al. 2010c). The *Fermi* data of M82 (filled circles) and NGC 253 (open circles) are obtained by Abdo et al. (2010a). The data in the very high-energy range of M82 (filled triangles, VERITAS Collaboration 2009) and NGC 253 (open triangles, Acero et al. 2009) are also plotted. The solid curves are the model spectra used to calculate EGRB (see text for details).

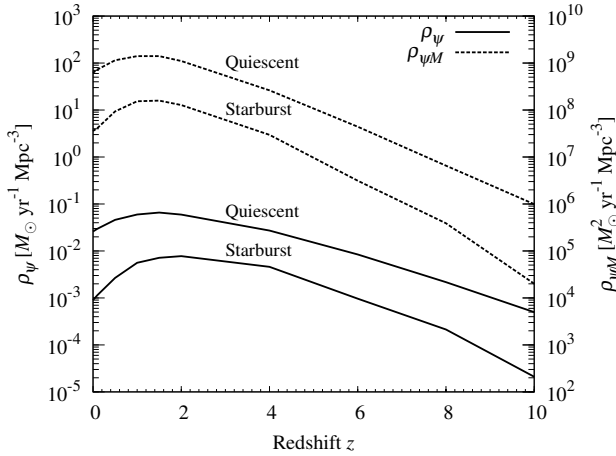


Figure 3. The evolution of the comoving densities of SFR (ρ_ψ , solid line) and the product of SFR and gas mass ($\rho_{\psi M}$, dashed line) in galaxies, calculated by the model of hierarchical galaxy formation. See the left and right ordinates for the units of ρ_ψ and $\rho_{\psi M}$, respectively.

hanced at high energy range of $\epsilon_\gamma \gtrsim 10$ GeV when the MW+power-law spectra is applied. However, the difference is not significant in the total EGRB flux from all star-forming galaxies, provided that quiescent galaxies have similar gamma-ray spectra to that of MW. It should also be noted that the classification of quiescent and starburst galaxies in the Mitaka model is determined to reproduce the optical/infrared observed properties of galaxies. Therefore the classification can be systematically different if we do it by the difference of gamma-ray spectra. This is an interesting question but difficult to answer at the present time because of too few observed data of gamma-ray spectra of galaxies.

The EGRB photon flux from all star-forming galaxies is 9.9×10^{-7} (escape limit) and 5.6×10^{-7} (calorimetric limit)

photons $\text{cm}^{-2} \text{s}^{-1} \text{sr}^{-1}$ (> 100 MeV), which are $7.0 \pm 1.8\%$ and $3.9 \pm 1.0\%$ of the EGRB flux observed by *Fermi* (including resolved sources), respectively. If we compare these results with the recent *Fermi* measurement of the unresolved EGRB flux, the contribution from star-forming galaxies become $9.6 \pm 2.4\%$ (escape limit) and $5.4 \pm 1.4\%$ (calorimetric limit). Here the error is that coming from the statistical 1σ error of the fitting formula of L_γ [eqs. (1) and (2)].

As a result of calculation the EGRB flux from star-forming galaxies in the calorimetric limit becomes lower than the escape limit. This seems counter-intuitive, since more gamma-rays should be produced in the calorimetric limit if the cosmic-ray energy input is fixed. This is because we use the datapoints of SMC and LMC to derive eq. (2). These galaxies are likely in the escape limit, making the slope of ψ - L_γ relation steeper. It would be an overestimate of EGRB if we calculate the “truly” calorimetric case, i.e., $L_\gamma \propto \psi^1$ with the proportionality constant for starburst galaxies. Rather, what we calculated here is the best empirical estimate of EGRB in a model in which L_γ is a function of ψ .

3.2. Redshift Distribution of EGRB Photons

Figure 6 shows the cumulative redshift distribution of the EGRB photons from star-forming galaxies. It is clearly seen in the figure that more than half of the total EGRB flux comes from galaxies at $z < 1$, and more than 90% from $z < 2$ both for the escape- and calorimetric-limit models. This is a reasonable result given the evolution of ρ_ψ and $\rho_{\psi M}$ as discussed in §2.4. The distribution of photons from starburst galaxies extend to slightly larger redshifts than that from quiescent galaxies, because of the stronger evolution of $\rho_{\psi M}$ at $z \sim 0-1$. Our result of the escape-limit can be compared with that of Ando & Pavlidou (2009, hereafter AP09). The two models are in rough agreement, though the median redshift of our model is slightly smaller than that of AP09. This may be because AP09 assumes that all the mass in the present-day stars contributes to gamma-ray production as gas in the early universe, while only a small fraction is in the form of cooled gas in our model, as discussed in §1.

3.3. Detectability of Nearby Star-Forming Galaxies

We also calculated the number of galaxies that are detectable by *Fermi*. The 1-yr sensitivity of *Fermi* is $\sim 3 \times 10^{-9}$ photons $\text{cm}^{-2} \text{s}^{-1}$ at $\epsilon_\gamma > 100$ MeV (Atwood et al. 2009). Our model predicts 4.6 and 2.3 galaxies above this flux in the escape- and calorimetric-limit models, respectively. These numbers are consistent with the actual number of four (SMC, LMC, M82, and NGC 253) or two (when SMC and LMC are excluded because it is within our Galaxy halo; see below). This result gives another support to the reliability of our EGRB prediction. However, it should be noted that in this estimate all galaxies in the Mitaka model are assumed to distribute randomly in space with a uniform mean density, because the clustering information of galaxy distribution is not included in the semi-analytic models like the Mitaka model. The density fluctuation and clustering in the local group around MW should affect the above estimate, especially for satellite galaxies like LMC. Not only the clustering effect but also the realistic detection efficiency of *Fermi* sources around the detection limit must be properly taken into account in a more quantitative analysis, which is beyond the scope of this paper. In the future, *Fermi* sensitivity will reach $\sim 1 \times 10^{-9}$ photons $\text{cm}^{-2} \text{s}^{-1}$ (> 100 MeV) by the 10-year observation, and we expect that *Fermi* will detect ~ 24

(escape limit) or 12 (calorimetric limit) nearby star-forming galaxies, though it is again subject to the uncertainty about clusting, and is probably optimistic assuming 100% detection efficiency above that flux.

Since the *Fermi* sensitivity becomes worse for extended sources than that for point sources, we checked the size of galaxies computed by the Mitaka model. There is a large scatter in the correlation between size and gamma-ray luminosity, but the average angular size of model galaxies brighter than *Fermi* 1-yr sensitivity is ~ 0.05 deg, which is much smaller than the *Fermi* angular resolution (~ 0.6 deg at 1 GeV, Atwood et al. 2009). Therefore the effect of extended sources should not significantly affect the above estimate for the number of detectable sources. It should also be noted that the size of an active star-forming region in a galaxy can be much smaller than that of the stellar disk of the same galaxy, as inferred from observations of NGC 253 (Acero et al. 2009). Therefore gamma-ray emitting regions can be much smaller than the size of the model galaxies in the Mitaka model.

4. DISCUSSION

4.1. Uncertainties

Here we examine the uncertainties about our estimate of the star-forming galaxy contribution to EGRB. As described in §2.2, we have calculated gamma-ray luminosity of galaxies by the relations $L_\gamma \propto (\psi M_{\text{gas}})^{0.86}$ and $L_\gamma \propto (\psi)^{1.2}$ which are obtained by the fit to the data of SMC, LMC, M82, and NGC 253. We also tested the cases of $L_\gamma \propto (\psi M_{\text{gas}})^1$ and $L_\gamma \propto (\psi)^1$, and in this case, the best-fit relations to the data becomes

$$L_\gamma = (0.36 \pm 0.08) \times \left(\frac{\psi}{M_\odot \text{ yr}^{-1}} \times \frac{M_{\text{gas}}}{10^9 M_\odot} \right) [10^{39} \text{ erg/s}], \quad (4)$$

and

$$L_\gamma = (0.28 \pm 0.08) \times \left(\frac{\psi}{M_\odot \text{ yr}^{-1}} \right) [10^{39} \text{ erg/s}]. \quad (5)$$

The eq. (4) is consistent with the estimate of the same relation by Pavlidou & Fields (2001) within the uncertainty of the conversion of MW supernova rate into SFR. We found that in these cases the EGRB flux becomes slightly different from our standard models: $9.3 \pm 2.0\%$ (escape limit) and $1.8 \pm 0.5\%$ (calorimetric limit) contribution to the observed total *Fermi* EGRB flux (or $12.8 \pm 2.8\%$ and $2.5 \pm 0.7\%$ against the unresolved component of EGRB reported by *Fermi*). The value of $12.8 \pm 2.8\%$ can be compared with another recent result by Fields et al. (2010), based on more empirical calculations about galaxy evolution, and they are consistent with each other within the systematic uncertainties.

Estimate of SFR is generally affected by the treatment of extinction by interstellar dust. The SFRs of LMC and SMC were estimated by their $H\alpha$ luminosities without extinction correction. If a part of ionizing photons are absorbed by dust before hydrogen ionization, their energy is converted into IR luminosity. Therefore, the sum of SFRs estimated by $H\alpha$ and IR luminosity gives a good upper bound on the total SFR. (It is an upper bound because non-ionizing photons also contribute to IR luminosity when they are absorbed by dust.) The SFRs estimated by IR luminosities of SMC and LMC are 0.0153 ± 0.0046 and $0.146 \pm 0.04 M_\odot/\text{yr}$, respectively, by the

same method as for SFR estimates of M 82 and NGC 253 described in §2.2. These are 40–60% of SFRs by $H\alpha$, indicating that these galaxies are not heavily obscured by dust. When we add the SFRs estimated by IR luminosity to the SFRs of SMC and LMC, the EGRB flux from star-forming galaxies changes slightly by a factor of 1.2. On the other hand, starburst galaxies (M82, NGC 253) have large extinctions and hence SFRs estimated by IR luminosity are much bigger than those by $H\alpha$, as mentioned in §2.2.

In the previous version of this paper put on the preprint server (arXiv:1005.1390v1), we reported about 14% contribution from star-forming galaxies to the total EGRB flux, which is about two times bigger than our new result. We examined the reason for this, and found that it is mainly due to the smaller SFR of LMC used in the previous version, which was estimated only by IR luminosity. As mentioned above, SFR from $H\alpha$ luminosity is about two times larger than that from IR for LMC and SMC. (Adding SMC to the nearby sample is also a new point of the current version, but it does not significantly affect the EGRB flux.) Therefore we believe that our new result is more appropriate, but it would be better to consider that the systematic uncertainty of the EGRB flux from star-forming galaxies is not smaller than a factor of two, given the small number of nearby galaxies with observed gamma-ray luminosities and uncertainties in estimates of SFR and gas mass.

4.2. Implications for the Origin of EGRB

Our result indicates that about 10% of EGRB can naturally be explained by star-forming galaxies. Here we discuss the origin of EGRB in general, also considering the larger contribution from AGNs. In Figs. 4 and 5, we plotted the EGRB model of AGNs by Inoue & Totani (2009, hereafter IT09). The IT09 model includes two populations of AGNs: one is blazars, and the other is non-blazars that are responsible for the EGRB at 1–10 MeV. Here we plotted models of $U03(q, \gamma_1)$ and $\Gamma = 3.5$ (see IT09 for details).

Many blazars have been detected by EGRET and *Fermi*, and it is obvious that they are the major contributor to EGRB. The blazar component of IT09 can account for 43% of the total EGRB flux, which is in good agreement with the latest observational estimate of Abdo et al. (2010d) based on the latest *Fermi* data³. Therefore, adding the component from star-forming galaxies, more than 50% of EGRB can be explained by the sum of surely existing sources. The non-blazar AGN component of IT09 has not yet been confirmed by observations, but it is introduced to explain the background radiation from hard X-ray to MeV region in a physically natural way (Inoue et al. 2008). If this component extends to ~ 100 MeV, the contribution to EGRB flux at >100 MeV could be $\sim 20\%$, and hence it is not difficult to explain $\gtrsim 70\%$ of EGRB by theoretically reasonable sources. It should also be noted that both the AGN component and star-forming galaxy component have remarkably similar spectra to the observed *Fermi* EGRB.

The $\lesssim 30\%$ residual of EGRB may not be explained simply by the sum of AGNs and star-forming galaxies, and there may be a room for different populations such as galaxy clusters or dark matter annihilation. However, there are still uncertainties

³ Note that the number (16%) quoted by Abdo et al. (2010d) is the fraction of unresolved blazars against the unresolved diffuse EGRB observed by *Fermi*. If this number is converted to that of all blazars against the total (unresolved + resolved components) EGRB flux, it increases to $\sim 40\%$ in good agreement with IT09.

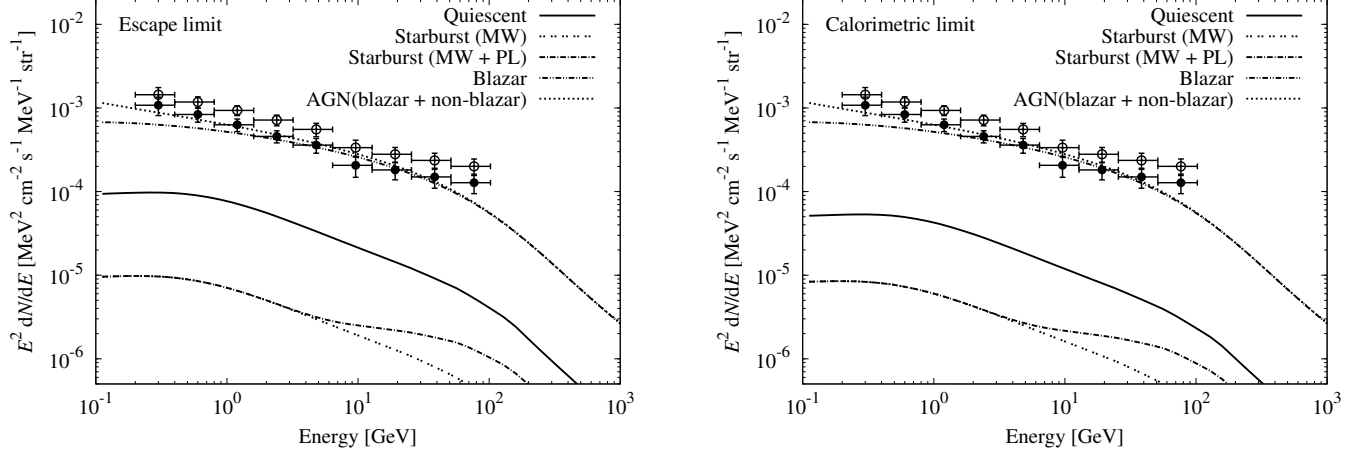


Figure 4. The EGRB spectrum. The theoretical predictions for the contributions from quiescent and starburst galaxies are separately shown, for the escape-limit (left panel) and the calorimetric limit (right). For starburst galaxies, we plotted two cases corresponding to two different spectral shapes of MW and MW + power-law. For comparison, the EGRB models of blazars and all AGNs (blazar + non-blazar) by Inoue & Totani (2009) are also shown. Open circles show the total EGRB flux reported by *Fermi* (Abdo et al. 2010c) including resolved sources, and the filled circles are the same but for the unresolved diffuse flux excluding resolved sources. The model curves should be compared with the open circle data.

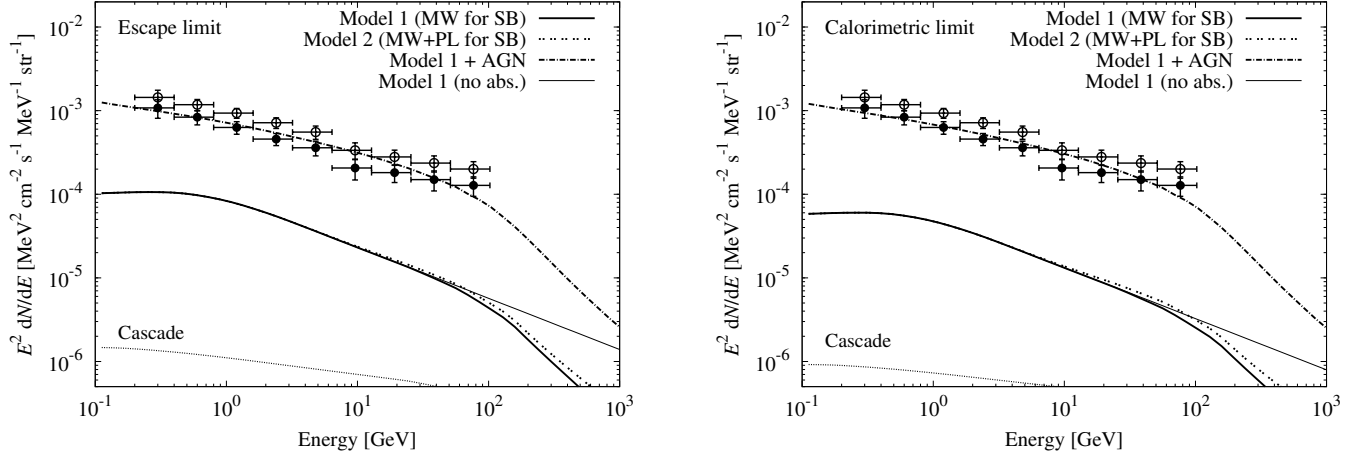


Figure 5. The same as Fig. 4, but for the sums of each component are shown. The Models 1 and 2 are EGRB from all star-forming galaxies (quiescent plus starburst), with the two different spectra for starbursts. To show the effect of intergalactic absorption, the Model 1 without absorption (thin solid line) and the cascade component of the Model 1 are also shown. The total of star-forming galaxies plus AGNs is also shown using the Model 1 for star-forming galaxies.

in the modeling of AGN gamma-ray luminosity function. The blazar luminosity function of IT09 was based on EGRET data, including uncertainties about detection and identification efficiencies depending on the location in the sky. The recent observational estimate of the blazar contribution by *Fermi* data includes a large correction about detection efficiency near the sensitivity limit, which is generally dependent on models. Blazars are highly variable sources, and it should add another uncertainty in EGRB estimates. Therefore we conclude that a large part of EGRB can be explained by known or physically reasonable sources, and there is no strong evidence for exotic components like dark matter annihilation.

5. CONCLUSIONS

We have presented a new calculation of EGRB from cosmic-ray interactions in star-forming galaxies, based on a state-of-the-art galaxy formation model in the framework

of hierarchical structure formation. The galaxy formation model is quantitatively consistent with various observations at high redshifts as well as the local universe. Gamma-ray luminosities of galaxies are calculated by star formation rate and gas mass in model galaxies, with the relation $L_\gamma \propto (\psi M_{\text{gas}})^{0.86}$ (the escape limit) or $L_\gamma \propto (\psi)^{1.2}$ (the calorimetric limit) which are calibrated by the recent observational data of nearby galaxies. The predicted number of nearby galaxies that are detectable by *Fermi* is consistent with the actual number observed so far.

We found that star-forming galaxies make 4–7% contribution to the total EGRB flux reported by *Fermi* in our standard model. Combined with the contribution from blazars as estimated by the *Fermi* data, more than $\sim 50\%$ of EGRB can be accounted for. If the soft power-law tail of CXB is extending from MeV to GeV region as expected from the MeV background data and theoretical considerations of AGN

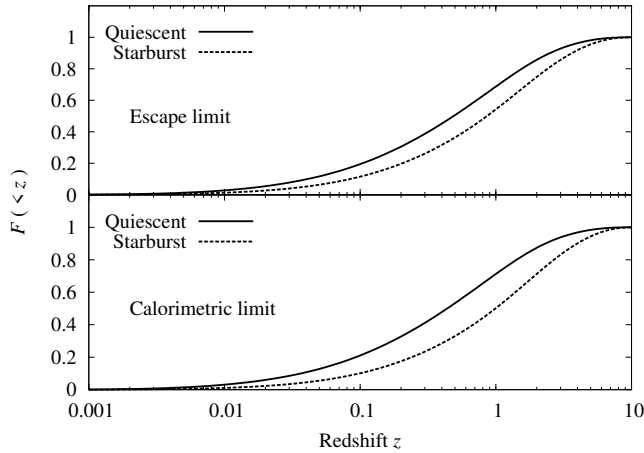


Figure 6. Cumulative redshift distribution of the EGRB photons (0.1–5 GeV) from star-forming galaxies. Quiescent and starburst galaxies are separately shown by solid and dashed curves, respectively.

accretion disks (Inoue et al. 2008), additional $\sim 20\%$ can be explained. The combined spectrum by AGNs and star-forming galaxies is remarkably similar to the observed EGRB spectrum. It should be noted that there is no free parameters that can be tuned to fit the observed EGRB spectrum in the present model; the blazar EGRB spectrum of IT09 is determined by the spectral templates of the blazar SED (spectral energy distribution) sequence, and that of the star-forming galaxy component in the present work by templates constructed by observed nearby galaxies. Therefore we conclude that a large part ($\gtrsim 70\%$) of EGRB can be explained by reasonable sources of AGNs and star-forming galaxies. Further examination is required to see whether the apparent $\lesssim 30\%$ residual of EGRB is mainly a result of modeling uncertainties, experimental/observational uncertainties in deriving the EGRB data, or significant contributions from completely different source populations. Given the good spectral agreement of the *Fermi* data and AGNs/star-forming galaxies, the rest of EGRB is also likely dominated by astrophysical sources accelerating particles, even if a completely different population is responsible for it.

It is in contrast that a large part of the blazar component of EGRB will be resolved into discrete sources by the ultimate *Fermi* sensitivity in the near future (IT09), while almost all of the star-forming galaxy component will remain unresolved because of the faintness of individual sources. Therefore, any exotic contribution like dark matter annihilation cannot be probed directly under the level of the star-forming galaxies, i.e., $\sim 10\%$ of the total EGRB flux. Another approach such as utilizing anisotropy would be required to search for the signal under that level (see, e.g. Ando et al. 2007; Siegal-Gaskins & Pavlidou 2009; Hensley et al. 2009; Cuoco et al. 2010)

We assumed a simple empirical relation between gamma-ray luminosity, SFR, and gas mass of galaxies. Only two spectral templates were used in the calculation. A next step would be to construct a more physical model of gamma-ray luminosity and spectrum based on a larger number of physical quantities (e.g., size and stellar radiation field in addition to SFR and gas mass), taking into account propagation of cosmic-rays and production processes of gamma-rays.

We would like to thank the anonymous referee for many

useful comments. This work was supported by the Grant-Aid for the Global COE Program "The Next Generation of Physics, Spun from University and Emergence" from the Ministry of Education, Culture, Sports, Science and Technology (MEXT) of Japan. The numerical calculations were in part carried out on SGI Altix3700 BX2 at Yukawa Institute for Theoretical Physics of Kyoto University. TT was supported by the Grant-in-Aid for Scientific Research (19047003, 19740099, 2004005) from MEXT. MARK was supported by the Research Fellowship for Young Scientists from the Japan Society for the Promotion of Science (JSPS).

REFERENCES

- Abdo, A. A., et al. 2010a, *ApJ*, 709, L152
— 2010b, *A&A*, 512, A7
— 2010c, *Phys. Rev. Lett.*, 104, 101101
— 2010d, *ApJ*, 720, 435
— 2010e, arXiv:1008.2127v1
Acero, F., et al. 2009, *Science*, 326, 1080
Aharonian, F. A., Coppi, P. S., & Voelk, H. J. 1994, *ApJ*, 423, L5
Atwood, W. B., et al. 2009, *ApJ*, 697, 1071
Ando, S., Komatsu, E., Narumoto, T., Totani, T. 2007, *Phys. Rev. D* 75, 3519
Ando, S., & Pavlidou, V. 2009, *MNRAS*, 400, 2122
Baugh, C.M., Lacey, C. G., Frenk, C. S., Granato, G.L., Silva, L., Bressan, A., Benson, A.J., & Cole, S. 2005, *MNRAS*, 356, 1191
Bhattacharya, D., & Sreekumar, P. 2009, *Research in Astronomy and Astrophysics*, 9, 509
Boissier S., & Prantzos, N. 1999, *MNRAS*, 307, 857
Brüns, C., et al. 2005, *A&A*, 432, 45
Cole, S., Aragon-Salamanca, A., Frenk, C. S., Navarro, J. F., & Zepf, S. E. 1994, *MNRAS*, 271, 781
Cuoco, A., Sellerholm, A., Conrad, J., & Hannestad, S. 2010, arXiv:1005.0843
Dale, D. A., et al. 2007, *ApJ*, 655, 863
Dale, D. A., & Helou, G. 2002, *ApJ*, 576, 159
Dar, A., & Shaviv, N. J. 1995, *Phys. Rev. Lett.*, 75, 3052
Dermer, C. D. 2007, *AIPC*, 921, 122
Diehl, R., et al. 2006, *Nature*, 439, 45
Fan, Y. Z., Dai, Z. G., & Wei, D. M. 2004, *A&A*, 415, 483
Fichtel, C. E., Hartman, R. C., Kniffen, D. A., Thompson, D. J., Ogelman, H. B., Ozel, M. E., & Tumer, T. 1977, *ApJ*, 217, L9
Fichtel, C. E., Simpson, G. A., & Thompson, D. J. 1978, *ApJ*, 222, 833
Fields, B. D., Pavlidou, V., & Prodanovic, T. 2010, *ApJ*, 722, L199
Fioc, M., Rocca-Volmerange, B. 1997, *A&A*, 326, 950
Franceschini, A., Rodighiero, G., Vaccari, M. 2008, *A&A*, 487, 837
Freedman, W. L., et al. 1994, *ApJ*, 427, 628
Hensley, B. S., Siegal-Gaskins J. M., Pavlidou, V. 2009, arXiv:0912.1854v2
Hilditch, R. W., Howarth, I. D., & Harries, T. J. 2005, *MNRAS*, 357, 304
Huchtmeier, W., & Richter, O. 1989, *A General Catalog of H I Observations of Galaxies* (New York: Springer)
Inoue, Y., Totani, T., & Ueda, Y. 2008, *ApJ*, 672, 5
Inoue, Y., & Totani, T. 2009, *ApJ*, 702, 523 (IT09)
Karachentsev, I. D., et al. 2003, *A&A*, 404, 93
Kashikawa, N., et al. 2006, *ApJ*, 648, 7
Kauffmann, G., White, S. D. M., & Guiderdoni, B. 1993, *MNRAS*, 264, 201
Kennicutt, Jr., R. C. 1998, *ApJ*, 498, 541
Kennicutt, R. C., Jr., Lee, J. C., Funes, S. J., José G., Sakai, S., & Akiyama, S. 2008, *ApJS*, 178, 247
Kneiske, T. M., Bretz, T., Mannheim, K., & Hartmann, D. H. 2004, *A&A*, 413, 807
Kneiske, T. M., & Mannheim, K. 2008, *A&A*, 479, 41
Knudsen, K. K., Walter, F., Weiss, A., Bolatto, A., Riechers, D. A., & Menten, K. 2007, *ApJ*, 666, 156
Kobayashi, M. A. R., Totani, T., & Nagashima, M. 2007, *ApJ*, 670, 919
— 2010, *ApJ*, 708, 1119
Lacki, B. C., Thompson, T. A., Quataert, E., Loeb, A., & Waxman, E. 2010, arXiv:1003.3257v1
Lichti, G. G., Bignami, G. F., & Paul, J. A. 1978, *Ap&SS*, 56, 403
Luks, Th., & Rohlfs, K. 1999, *A&A*, 263, 41
Nagashima, M., Gouda, N., & Sugiura, N. 1999, *MNRAS*, 305, 44
Nagashima, M., Yahagi, H., Enoki, M., Yoshii, Y., & Gouda, N. 2005, *ApJ*, 634, 26
Nagashima, M., & Yoshii, Y. 2004, *ApJ*, 610, 23
Orear, J. 1981, *AmJPh*, 50, 912
Pavlidou, V., & Fields, B. D. 2001, *ApJ*, 558, 63
Pavlidou, V., & Fields, B. D. 2002, *ApJ*, 575, L5
Pence, W. D. 1980, *ApJ*, 239, 54
Pietrzyński, G., et al. 2009, *ApJ*, 697, 862
Salamon, M. H., & Stecker, F. W. 1998, *ApJ*, 493, 547
Salim, S., et al. 2009, *ApJ*, 700, 161
Sanders, D. B., Mazzarella, J. M., Kim, D., Surace, J. A., & Soifer, B. T. 2003, *AJ*, 126, 1607

- Siegal-Gaskins, J. M., & Pavlidou, V. 2009, *Phys. Rev. Lett.*, 102, 241301
Somerville, R. S., & Primack, J. R. 1999, *MNRAS*, 310, 1087
Springob, C. M., Haynes, M. P., Giovanelli, R., & Kent, B. R. 2005, *ApJS*, 160, 149
Sreekumar, P., et al. 1992, *ApJ*, 400, L67
—. 1998, *ApJ*, 494, 523
Stanimirović, S., Staveley-Smith, L., Dickey, J. M., Sault, R. J., & Snowden, S. L. 1999, *MNRAS*, 302, 417
Staveley-Smith, L., Kim, S., Calabretta, M. R., Haynes, R. F., & Kesteven, M. J. 2003, *MNRAS*, 339, 87
Stecker, F. W., Malkan, M. A., & Scully, S. T. 2006, *ApJ*, 648, 774
Strong, A. W., Wolfendale, A. W., & Worrall, D. M. 1976, *MNRAS*, 175, 23
Strong, A. W., Moskalenko, I. V., & Reimer, O. 2000, *ApJ*, 537, 763
—. 2004a, *ApJ*, 613, 956
—. 2004b, *ApJ*, 613, 962
Thompson, T. A., Quataert, E., & Waxman, E. 2007, *ApJ*, 654, 219
Torres, D. F., Reimer, O., Domingo-Santamaría, E., & Digel, S. W. 2004, *ApJ*, 607, 99
Totani, T., & Takeuchi, T. T. 2002, *ApJ*, 570, 470
Venters, T. M. 2010, *ApJ*, 710, 1530
VERITAS Collaboration 2009, *Nature*, 462, 770
Weiß, A., Walter, F., & Scoville, N. Z. 2005, *A&A*, 438, 533
Westerlund, B.E. 1997, *The Magellanic Clouds*, (Cambridge: Cambridge Univ. Press), 28